Expansion of a distinct cytotoxic CD4 T_{FH}-cell cluster in lymph nodes of patients with complicated common variable immunodeficiency

David Friedmann, PhD, Kathryn J. Payne, PhD, Victoria Cousin, MSc, Geoffroy Andrieux, PhD, Ke Meng, MMed, Alexandra Emilia Schlaak, MD, et al

GRAPHICAL ABSTRACT

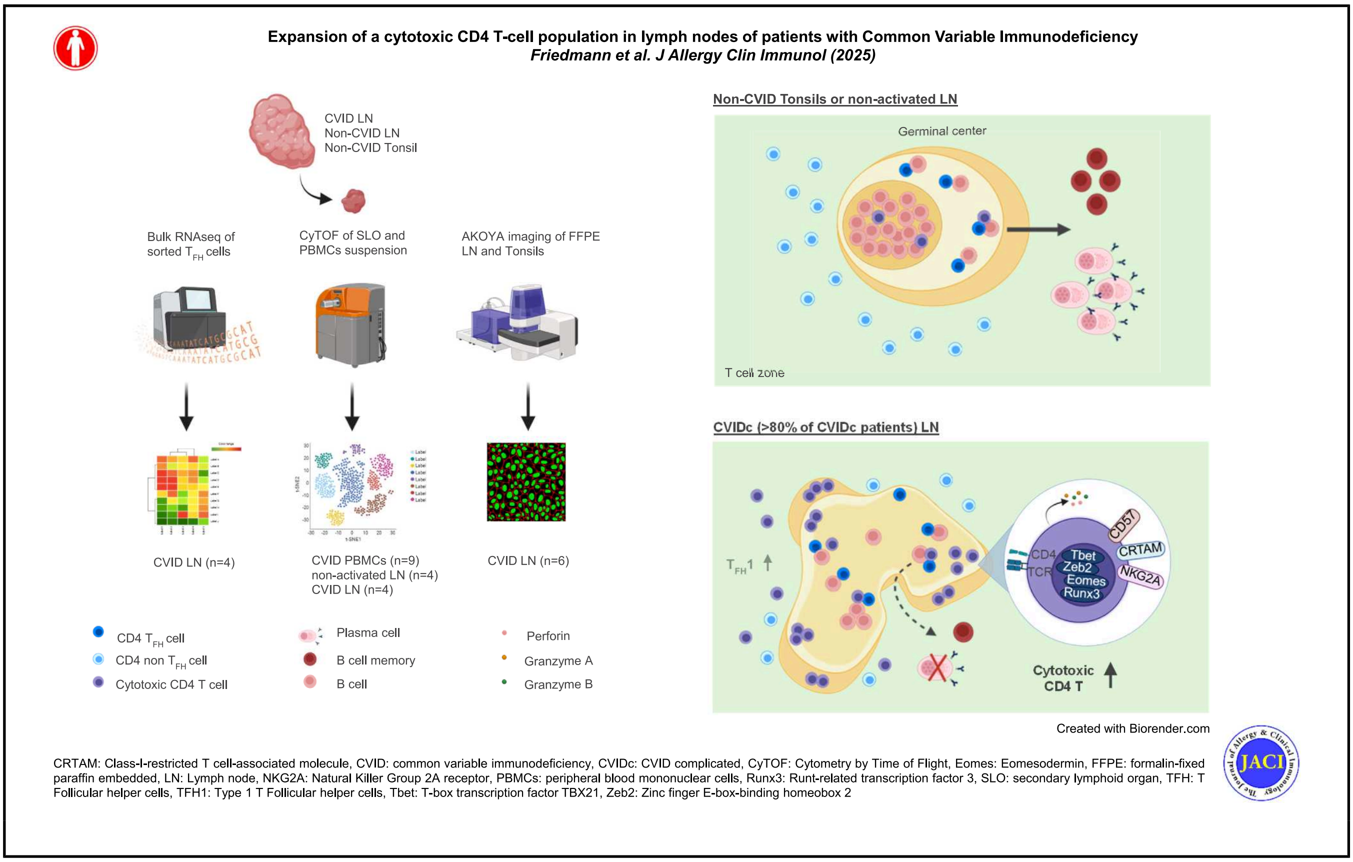

Capsule summary: Type 1 polarization of T_{FH} cells in complicated common variable immunodeficiency lymph nodes is associated with the expansion of activated cytotoxic CD4 T_{FH} cells in germinal centers, which might contribute to the humoral immunodeficiency and immune dysregulation in these patients.

J Allergy Clin Immunol 2025;■■■:■■■-■■■.

https://doi.org/10.1016/j.jaci.2025.09.032

Expansion of a distinct cytotoxic CD4 T_{FH}-cell cluster in lymph nodes of patients with complicated common variable immunodeficiency

David Friedmann, PhD,[a,b,c]* Kathryn J. Payne, PhD,[a,b,c]* Victoria Cousin, MSc,[a,b,c,d] Geoffroy Andrieux, PhD,[e] Ke Meng, MMed,[f] Alexandra Emilia Schlaak, MD,[f] Susanne Unger, PhD,[a,b,g] Adam Klocperk, MD, PhD,[a,b,h] Christoph Geier, MD,[a,b] Katja Gräwe, MTA,[i] Jens Pfeiffer, MD,[j] Till F. Jakob, MD,[j] Oliver Hausmann, MD,[k] Peter Anhut, MD,[l] Michelle Shabani, MD,[i] Konrad Kurowski, MD,[i] Manuel Rogg, MD,[i] Konrad Aumann, MD,[i] Maximilian Seidl, MD,[i,m] Jan Provaznik, MD,[n] Vladimir Benes, MD, PhD,[n] Melanie Boerries, PhD,[e,o] Tobias Boettler, MD, PhD,[f] Christoph Schell, MD, PhD,[i] Sigune Goldacker, MD,[a,b] Baerbel Keller, PhD,[a,b] Bertram Bengsch, MD, PhD,[f,o,p] and Klaus Warnatz, MD[a,b] *Freiburg, Kronach, Düsseldorf, and Heidelberg, Germany; Zurich and Luzern, Switzerland; and Prague, Czech Republic*

Background: Patients with common variable immunodeficiency (CVID) suffer from hypogammaglobulinemia linked to an inadequate differentiation of long-lived humoral immunity and an impaired germinal center (GC) response in most cases.
Objective: We sought to further characterize the transcriptome and phenotype of T follicular helper (T_{FH}) cells of patients with complicated CVID (CVIDc) as key players in the GC reaction.
Methods: Sorted T_{FH} cells from CVIDc lymph nodes and non-CVID immunocompetent tonsils were analyzed by bulk RNA sequencing. Altered protein expression was verified by comparison with non-CVID tonsils and lymph nodes using cytometry by time-of-flight analysis. Tissue localization of cells was determined by multifluorescence imaging.
Results: Transcriptome analysis of sorted T_{FH} cells revealed an enrichment of cytotoxicity-associated gene sets in patients with CVIDc. Extended immune phenotyping identified different cytotoxic CD4 memory populations expressing T-bet, EOMES (eomesodermin), class I–restricted T-cell–associated molecule, perforin, and granzymes. One cluster coexpressing markers of T_{FH} differentiation C-X-C chemokine receptor type 5, inducible costimulator, and programmed cell death protein 1 was expanded in CVIDc lymph nodes. Histologic sections confirmed the increase in Granzyme-B$^+$EOMES$^+$CD4 cells within GCs of patients' lymph nodes. Only few of these cells circulate in peripheral blood.
Conclusions: Our study reports for the first time that the type 1 polarization in lymph nodes of patients with CVIDc is associated with an expansion of a distinct cytotoxic CD4 T_{FH}-cell cluster within GCs, which is only poorly reflected in peripheral blood. Because a detrimental role of these cells has been implied in the context of autoimmunity and chronic infection, further investigations are required to explore their role in the GC failure and immune dysregulation in patients with CVID. (J Allergy Clin Immunol 2025;■■■:■■■-■■■.)

Key words: *Common variable immunodeficiency, CVID, cytotoxicity, lymph node, CD4 T cells, T follicular helper cell, RNA-seq, CyTOF, type 1 polarization*

Common variable immunodeficiency (CVID), the most prevalent symptomatic human primary immunodeficiency, refers to an antibody deficiency syndrome of heterogeneous and mostly unknown pathogenesis. The hallmark of the disease is a reduction in serum IgG and IgA and impaired specific antibody responses.[1,2] Mutations in more than 20 genes have been associated with the clinical presentation of CVID, currently explaining about 20% of CVID cases.[3,4] According to the heterogeneous clinical presentation, the disease is commonly divided into 2 subgroups. Patients who suffer "only" from recurrent bacterial infections are classified as CVID infection only (CVIDio), and those with a more complicated disease phenotype, featuring manifestations of immune dysregulation, are classified as CVID complicated (CVIDc). These manifestations include noninfectious complications such as

From [a]the Division of Immunodeficiency, Department of Rheumatology and Clinical Immunology, and [b]the Center for Chronic Immunodeficiency, Medical Center - University of Freiburg, Faculty of Medicine, [c]the Faculty of Biology, [d]Spemann Graduate School of Biology and Medicine, and [e]the Institute of Medical Bioinformatics and Systems Medicine and [f]the Department of Medicine II (Gastroenterology, Hepatology, Endocrinology and Infectious Diseases), Medical Center - University of Freiburg, Faculty of Medicine, University of Freiburg, Freiburg; [g]the Institute of Experimental Immunology, University of Zurich, Zurich; [h]the Department of Immunology, 2nd Faculty of Medicine, Charles University and University Hospital in Motol, Prague; [i]the Institute for Surgical Pathology and [j]the Department of Oto-Rhino-Laryngology, Medical Center - University of Freiburg, Faculty of Medicine, University of Freiburg, Freiburg; [k]Löwenpraxis and Klinik St Anna, Luzern; [l]Medical Practice of Oncology, Kronach; [m]the Institute of Pathology, Heinrich Heine University and University Hospital of Düsseldorf, Düsseldorf; [n]the European Molecular Biology Laboratory, Genomics Core Facility, Heidelberg; [o]the German Cancer Consortium (DKTK), Partner site Freiburg (a partnership between DKFZ and Medical Center - University of Freiburg), Freiberg; and [p]Signalling Research Centres BIOSS and CIBSS, University of Freiburg, Freiburg.

*These authors contributed equally to this work.

Received for publication August 5, 2024; revised September 9, 2025; accepted for publication September 12, 2025.

Corresponding author: Klaus Warnatz, MD, Division of Immunodeficiency, Department of Rheumatology and Clinical Immunology, Medical Center - University of Freiburg, Faculty of Medicine, Breisacherstrasse 115, Freiburg 79106, Germany. E-mail: klaus.warnatz@uniklinik-freiburg.de.

0091-6749

https://doi.org/10.1016/j.jaci.2025.09.032

Abbreviations used

CRTAM:	Class I–restricted T-cell–associated molecule
CTLA-4:	Cytotoxic T-lymphocyte–associated antigen 4
CVID:	Common variable immunodeficiency
CVIDc:	Common variable immunodeficiency complicated
CVIDio:	Common variable immunodeficiency infection only
CXCR3/CXCR5:	C-X-C chemokine receptor type 3/5
CyTOF:	Cytometry by time of flight
DEG:	Differentially expressed gene
EOMES:	Eomesodermin
GC:	Germinal center
GZMA/B:	Granzyme A/B
NK:	Natural killer (cells)
NKG2A/7:	Natural killer cell granule protein 2A/7
PD-1:	Programmed cell death protein 1
SLO:	Secondary lymphoid organ
T_{FH}:	T follicular helper
TIGIT:	T-cell immunoreceptor with Ig and ITIM domains

autoimmune cytopenia, granulomatous disease, splenomegaly and lymphadenopathy, interstitial lung disease, enteropathy, and hepatopathy,[5] which frequently contribute to a significantly reduced quality of life and increased morbidity and mortality.[6-9]

The defining humoral immunodeficiency in CVID is associated with an altered B-cell homeostasis, which has been used for disease classification in EUROClass.[10] The severe reduction in circulating class-switched memory B cells and plasmablasts in most patients has suggested a defect of germinal centers (GCs) as the site of origin for both populations. Nevertheless, many patients, especially of the CVIDc subgroup, are still able to form GCs, which are however frequently transformed and irregularly shaped.[11,12]

More recent analysis of GCs of patients' lymph nodes demonstrated an increase in CXCR5 (C-X-C chemokine receptor type 5)-positive follicular CD8 T cells, associated with an exhaustion, senescence, and immunoregulatory phenotype, which was partly reflected in peripheral blood.[13,14]

To date, only a few studies have investigated CD4 T cells in secondary lymphoid tissues of patients with CVID. In the peripheral blood of many patients with CVIDc, recent thymic emigrants and naive CD4 T cells are reduced[15,16] and the memory CD4 compartment is shifted toward IFN-γ–producing T_H1 and circulating T follicular helper (T_{FH}) cells.[12] Memory CD4 T cells isolated from these patients show higher expression of inhibitory receptors including PD-1 (programmed cell death protein 1), LAG3 (lymphocyte activation gene 3), CTLA-4 (cytotoxic T-lymphocyte–associated antigen), and TIGIT (T-cell immunoreceptor with Ig and ITIM domains) but retain the capacity to produce IFN-γ and to proliferate.[17]

On the basis of our findings of a type 1 polarization affecting also lymph nodes of patients with CVIDc,[12,18] we wondered whether the type 1 polarization of T_{FH} cells in GCs of patients with CVIDc might be associated with an increased presence of cytotoxic T_{FH} cells and set out to characterize these cells by exploratory bulk RNA sequencing from lymph nodes of patients with CVID compared with tonsils of immunocompetent non-CVID controls. Our analysis revealed indeed an increased cytotoxic signature among memory CD4 T cells, which we were able to assign to a specific cluster of cytotoxic CD4 T_{FH} cells locating to GCs in secondary lymphoid tissues of patients with CVIDc.

METHODS

Cohort description

All procedures performed in this study were in accordance with the ethical standards of the institutional and national research committee and with the 1964 Helsinki Declaration and its later amendments. The study was approved by local authorities (Freiburg 251/13 and 254/19) and written informed consent was obtained from all individual participants before inclusion in the study. Lymph nodes (n = 6) in patients with CVID with lymphadenopathy were removed for diagnostic purposes to exclude lymphoma. Five patients belonged to the CVIDc subgroup and 1 to the CVIDio subgroup (for further details, see Table E1 in this article's Online Repository at www.jacionline.org). Control biopsies were obtained from either non-CVID tonsils (n = 7) or lymph nodes (n = 4) of subjects without known immunodeficiency undergoing tonsillectomy or lymph node extirpation, respectively. Tissues were included after the exclusion of lymphoma and other malignancies. Peripheral blood samples were obtained from 9 patients with CVID and 7 healthy adult volunteers. The experimental overview is provided in Tables E2 and E3 (in the Online Repository available at www.jacionline.org).

Isolation of mononuclear cells from peripheral blood and from secondary lymphoid organs

PBMCs were isolated by Ficoll density centrifugation (Pancoll; Pan-Biotech, Aidenbach, Germany). Mononuclear cells from lymph nodes and tonsils were isolated by mechanical disruption as described previously.[12] Cells were frozen in Iscove modified Dulbecco medium with 10% dimethyl sulfoxide and 40% FBS in liquid nitrogen until further use.

RNA sequencing and analysis

For RNA sequencing, T_{FH} cells were sorted from secondary lymphoid organ (SLO) mononuclear cells on the MoFlo Astrios (Beckman Coulter Life Sciences, Indianapolis, Ind) by gating on $CD3^+CD4^+CD45RA^-CXCR5^{hi}PD\text{-}1^{hi}$ T cells (Fig 1, *A*). RNA was isolated using the RNeasy Mini or Micro Kit (QIAGEN GmbH, Hilden, Germany) according to the manufacturer's instructions. Barcoded stranded mRNA-sequencing libraries were prepared from high-quality total RNA samples (200 ng/sample) using the TruSeq RNA Sample Preparation v2 Kit (Illumina, Inc, San Diego, Calif). Libraries were pooled in equimolar amounts, loaded on the Illumina sequencer NextSeq 500, and sequenced unidirectionally, generating approximately 500 million reads per sample, each 85 bases long. Adapter- and quality-trimming was performed with Trimmomatic v0.38 (Usadel Lab, RWTH Aachen University, Aachen, Germany),[19] and alignments and gene counts were obtained using STAR v2.5.2b[20] on GRCh38 genome and annotation (GRCh38.p7).

Genes that were quantified in more than 50% of the data set were selected. Differentially expressed genes (DEGs) were determined using the limma (v3.54.0) R (v4.2.2) package,[21] including library size and Trimmed Mean of M-values (TMM) normalizations. DEGs were defined by adjusted *P* values less than .05 and are provided in Table E4 (in the Online Repository available at www.jacionline.org).

Gene-set enrichment analysis was performed using the clusterProfiler (v4.6.0) R package[22] with the MSigDB gene-set

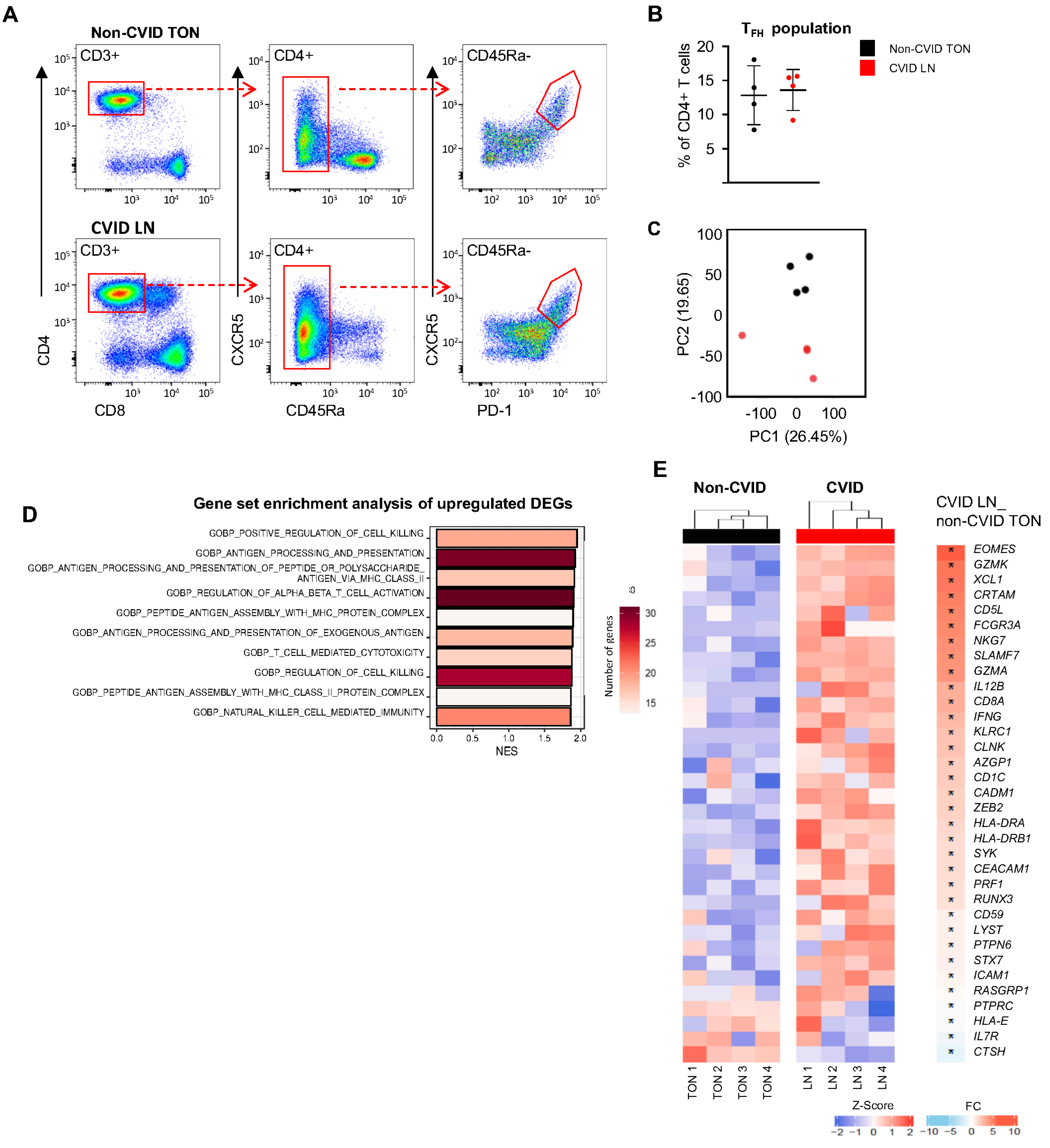

FIG 1. Enriched cytotoxicity-associated gene signature in T_{FH} cells of patients with CVIDc. **A,** Gating strategy for identification of T_{FH} cells gated on $CD3^+CD4^+CD45RA^-$ T cells in 1 representative non-CVID tonsil and 1 representative CVID lymph node. **B,** Statistical abundance of T_{FH} cells in $CD4^+$ T cells in secondary lymphoid tissues. **C,** Principal-component analysis on RNA-sequencing data showing separation of CVIDc lymph nodes (*red*) and non-CVID control tonsils (*black*). **D,** Gene-set enrichment barplot showing the normalized enrichment score for the top 10 upregulated GOBP in CVIDc vs non-CVID tissues. Color code indicates the number of genes in the leading edge. **E,** Gene-level heatmap showing the row-wise scaled (*z* score) mRNA expression and $\log_2$ fold change of significant genes involved in cytotoxicity. The asterisk (*) indicates significant regulation (adjusted $P < .05$) between CVIDc and non-CVID tissues. *GOBP,* Gene Ontology Biological Processes.

repository as reference.[23] Adjusted *P* values less than .05 (Benjamini-Hochberg method) were considered as significant.

Data are available from the Gene Expression Omnibus (accession no. GSE274117).

Mass cytometry

Single-cell suspensions were incubated with 20 μM lanthanum-139 (Trace Sciences)-loaded maleimido-mono-amine-1,4,7,10-tetraazacyclododecane-1,4,7,10-tetraacetic acid (DOTA) (Macrocyclics, Inc, Dallas, Tex) in PBS for 5 minutes at room temperature for live/dead discrimination. Cells were incubated with a mix of β2-microglobulin–based barcodes for 30 minutes at 4°C to minimize batch effects[24] and washed twice with staining buffer before pooling. Cells labeled with surface antibodies were incubated for 30 minutes at room temperature, washed twice, prefixed with 1.6% paraformaldehyde, washed, and then fixed and permeabilized using FoxP3 staining buffer set (Thermo Fisher Scientific – eBioscience, San Diego, Calif) to stain intracellularly for 60 minutes at room temperature. Cells were further washed before fixation in 4% paraformaldehyde (Electron Microscopy Sciences) solution containing 125 nM iridium overnight at 4°C.

After acquisition, CyTOF (cytometry by time of flight) files were normalized by bead-based Nolan Lab normalizer (EQ Four Element Calibration Beads, Standard BioTools, South San Francisco, Calif). Flow Cytometry Standard (FCS) files were processed by using FlowJoV10 Gaussian-derived parameters "Residual," "Beads," "Center," "Offset," "Width," "Event Length," and "Iridium" to eliminate dead cells, debris, and normalization beads before debarcoding. Batch effects were corrected by BatchAdjust. Further data analysis by FlowSOM[25] and Uniform Manifold Approximation and Projection (UMAP)[26] was performed using OMIQ (Dotmatics, Santa Fe, NM). For conventional gating and subsampling, $CD56^-CD19^-CD8^-CD45^+$ $CD3^+CD4^+$ T cells were used. Dimensionality reduction was performed on the remaining 39 markers. A list of all the antibodies used is provided in Table E5 (in the Online Repository available at www.jacionline.org).

Multiplex immunofluorescence imaging

Paraffin-embedded tissue sections (2 μm) were cut from 4% buffered formaldehyde-fixed samples and stained using the Opal Polaris 7 Kit (Akoya Biosciences, Inc, Marlborough, Mass) with antibodies and dilutions specified in Table E6 (in the Online Repository available at www.jacionline.org). Imaging was performed using the PhenoCycler-Fusion microscope (Akoya Biosciences, Inc). Regions of interest were selected and analyzed using QuPath.[27] For quantification of $EOMES^+$ (eomesodermin) $GZMB^+$ (granzyme B) $CD4^+$ T cells, 10 GCs and 10 T-cell zones were analyzed per sample (non-CVID tonsils, n = 4; CVID lymph nodes, n = 6).

Statistical analysis

Statistical significance was assessed with unpaired ordinary 1-way ANOVA for data sets with Gaussian distribution or with the nonparametric test for data sets without Gaussian distribution. Dot plots display each value reflecting their distribution.

Results were analyzed with GraphPad Prism software v9.5.0 (Dotmatics), and *P* values less than .05 were considered significant.

RESULTS

The transcriptome of T_{FH} cells shows an enrichment of cytotoxicity-related gene sets in CVIDc

Principal-component analysis of bulk RNA-sequencing data of sorted T_{FH} cells ($CD3^+CD8^-CD4^+CD45RA^-CXCR5^{hi}PD\text{-}1^{hi}$) from lymph nodes of patients with CVIDc (n = 4) and tonsils from non-CVID control individuals (n = 4) demonstrated a distinct clustering of CVIDc and control samples (Fig 1, *A-C*).

Unbiased primary analysis of all expressed transcripts revealed 2465 DEGs, with 1506 upregulated genes and 959 downregulated genes (adjusted $P < .05$; Table E4). These DEGs comprised *TIGIT*, transcription factors *EOMES* and *TBX21* (T-box transcription factor 21; encoding T-bet), and *GBP5* (guanylate binding protein 5), *ISG15* (interferon-stimulated gene 15), *CXCL10* (C-X-C motif chemokine ligand 10), or *IFNG* (data not shown), reflecting markers of exhaustion, an increased interferon signature, and T_H1 bias as previously demonstrated,[12] but additionally an enrichment of gene sets related to cytotoxicity based on the Gene Ontology Biological Processes database Fig 1, *D*).

The enriched DEGs related to cytotoxicity (Fig 1, *E*) comprised *RUNX3* (runt-related transcription factor 3),[27,28] *ZEB2* (zinc finger E-box binding homeobox 2),[29] and *CRTAM* (class I–restricted T-cell–associated molecule) and its ligand *CADM1* (cell adhesion molecule 1),[30] which denotes the $CD4^+$ cytotoxic T-lymphocyte lineage as well as *KLRC1* (killer cell lectin-like receptor C1; encoding NKG2A [natural killer cell granule protein 2A]) as a regulator of cytotoxicity in natural killer (NK) and CD8 T cells.[31] *XCL1* (X C-Ligand 1), a chemokine also known as lymphotactin, is produced by T and NK cells[32] as well as *SLAMF7* (signaling lymphocytic activation molecule family member 7), which not only promotes NK-cell degranulation[33] but is also described specifically in a cytotoxic $CD4^+$ T-cell population in IgG4-related disease.[34] Consistent with these findings, transcripts of molecules involved in the exocytosis of cytotoxic granules in lymphocytes such as *NKG7*[35] and *LYST* (lysosomal trafficking regulator)[36] as well as the content of cytotoxic granules perforin (*PRF1*) and granzyme A and granzyme K (*GZMA* and *GZMK*) and their release of *STX7* (syntaxin 7) were among the enriched DEGs of CVID-derived T_{FH} cells. To confirm this transcriptional signature on protein level and to delineate its cellular origin, we designed a CyTOF panel to characterize $CD4^+$ T cells in SLOs of patients with CVIDc and non-CVID controls, including markers of their cytotoxic nature.

CyTOF analysis identifies an expanded cytotoxic CD4 T_{FH}-cell cluster in CVIDc lymph nodes

The in-depth CyTOF analysis was performed on 4 lymph nodes of patients with CVIDc, 5 non-CVID tonsils, and 4 non-CVID lymph nodes using a 44-plex marker panel. Dimensionality reduction of the subsampled $CD19^-CD56^-$ $CD8^-CD45^+CD3^+CD4^+$ T cells was accomplished by UMAP using the remaining 38 nonlineage markers. Clustering of high-dimensional data by self-organizing map algorithm (FlowSOM) identified 29 unique clusters of CD4 T cells (Fig 2,

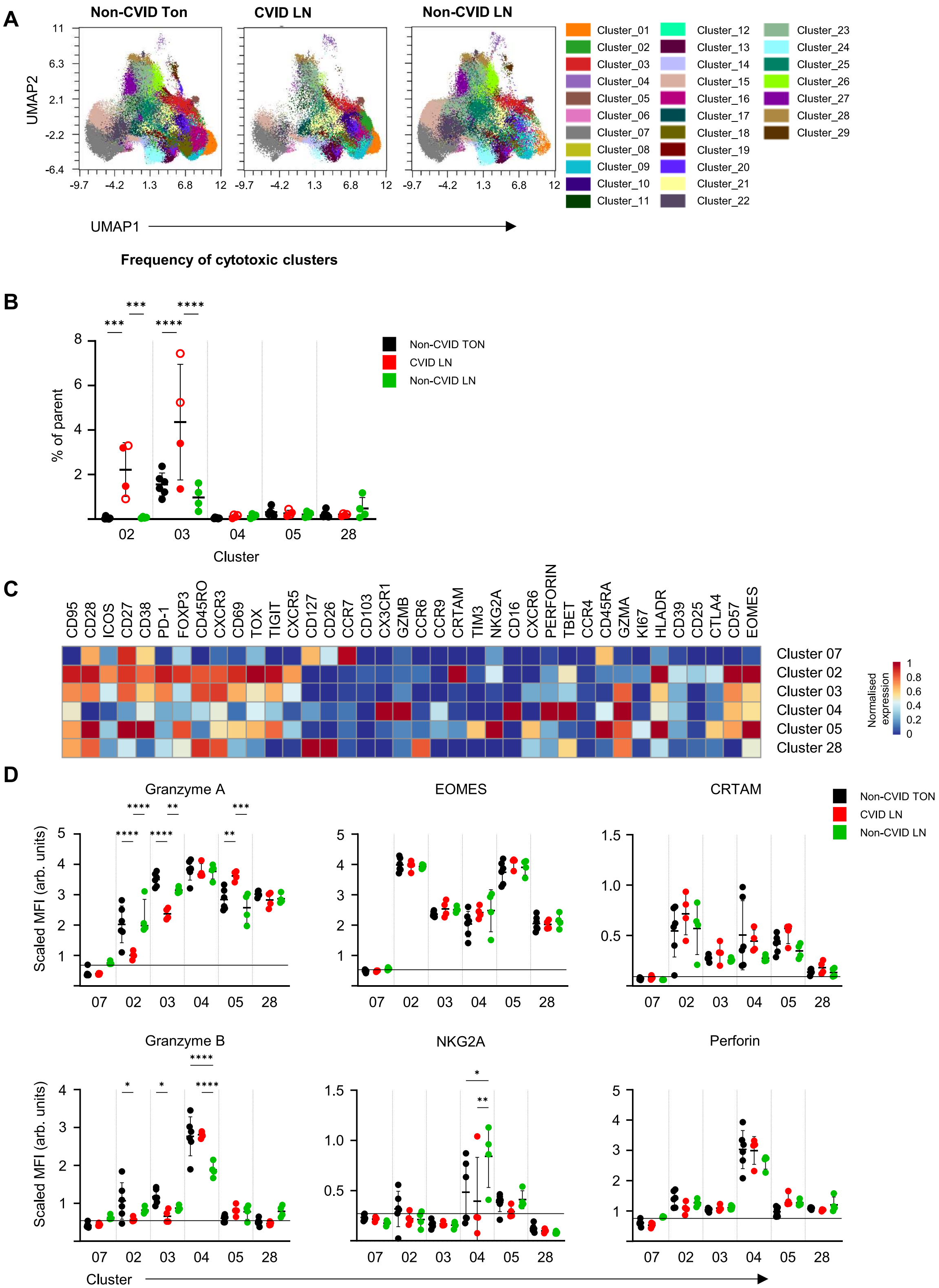

FIG 2. Increased abundance of 1 CD4^{+} T-cell cluster expressing cytotoxicity- and GC-associated markers in CVIDc lymph nodes. **A,** UMAP projection of unsupervised CyTOF analysis of non-CVID tonsils (n = 5), CVIDc lymph nodes (n = 4), and non-CVID lymph nodes (n = 4). Clusters of similar cells were identified using FlowSOM. **B,** Abundance of cytotoxic clusters of interest in CD4^{+} T cells (clusters 2, 3, 4, 5, and 28) in non-CVID tonsils (*black*), CVIDc lymph nodes (*red*), and non-CVID lymph nodes (*green*). *Open circles* represent patients under immunosuppressive treatment. **C,** Heatmap of scaled expression values of markers analyzed with mass cytometry in cytotoxic clusters of interest (clusters 2, 3, 4, 5, and 28) compared with naive cells (cluster 7). **D,** Expression of cytotoxic markers GZMA, EOMES, CRTAM, GZMB, NKG2A, and perforin in naive cells (cluster 7) and clusters of interest (clusters 2, 3, 4, 5, and 28). MFI axis values are scaled by arcsinh, measured in arbitrary units. The baseline represents the peak expression of the respective molecule in non-CVID naive T cells. *MFI*, Mean fluorescence intensitiy; *UMAP,* Uniform Manifold Approximation and Projection.

A) including CD45RA$^+$CCR7$^+$ naive cells in cluster 7 (see Fig E1, *A* and *B*, in this article's Online Repository at www.jacionline.org), which served as a control for the clusters of interest.

Focusing on cytotoxicity-associated markers GZMA, GZMB, EOMES, CRTAM, NKG2A, and perforin, 5 cytotoxic clusters of interest were identified, with cluster 2 and cluster 3 being significantly enriched in CVIDc lymph nodes (Fig 2, *B*). Although this increase did not associate with immunosuppressive treatment in cluster 2, the abundance of cluster 3 was higher in the 2 patients receiving steroid therapy. Because of the very low abundance of clusters 4, 5, and 28 (in both CVIDc and control tissues), the lack of difference in abundance, and the lack of markers of T_{FH}-cell differentiation such as ICOS (inducible costimulator), CXCR5, and PD-1, they were not considered a relevant source of the differential expression of cytotoxic signature (Fig 2, *C*). In contrast, especially cluster 2 expressed T_{FH} markers comparable with the expression in bona fide T_{FH} cells of cluster 1 (Fig E1, *C*). Cluster 3 did not sufficiently express these markers (Fig E1, *C*) and, therefore, cluster 2 was considered the potential source of the elevated cytotoxic mRNA signature in T_{FH} cells. Cluster 2 expresses additionally CXCR3 and T-bet as hallmarks of T_H1 differentiation (Fig 2, *C*). This cluster expresses very high levels of EOMES and CRTAM comparable with the control tissue, whereas the detectable GZMA and GZMB expression was decreased in CVID-derived cells when compared with control cells (Fig 2, *C* and *D*). This can be due to either loss of expression during active degranulation or low production due to chronic exhaustion. To distinguish the 2 potential explanations, we investigated the surface expression of CD107a as an indicator for concurrent degranulation *ex vivo* without additional stimulation (see Table E7 in this article's Online Repository at www.jacionline.org). In both CVIDc lymph node samples that were available for this analysis, we could demonstrate increased CD107a surface expression on unstimulated CD4 T cells of CVIDc versus non-CVID tissues, suggesting an ongoing degranulation activity of these cells at the time of removal in contrast to a stage of chronic exhaustion (Fig E1, *D*). Consistent with this, cluster 2 additionally expressed elevated levels of markers associated with recent T-cell receptor–mediated activation such as enhanced expression of HLA-DR, CD25, and TIGIT. In the same context, we interpreted the elevated FoxP3 expression, which still remained below the level of cluster 13 assigned as containing regulatory T cells (Fig E1, *E*).

In summary, this CyTOF analysis identified 5 distinct cytotoxic CD4$^+$ T-cell clusters, 2 of which were more abundant in CVIDc and cluster 2 expressing additional markers compatible with GC homing.

Cytotoxic CD4 T cells locate within GCs of CVID lymph nodes

To confirm an increased localization of cytotoxic CD4 T cells within GCs of SLOs, we performed a multiplex immunofluorescence staining of formalin-fixed paraffin-embedded slides of lymph nodes of patients with CVID (n = 6, including 1 patient with CTLA-4 haploinsufficiency and 1 patient with CVIDio) and tonsils from non-CVID controls (n = 4) (Fig E2, *A*). Follicular and extrafollicular structures in all samples were identified using CD20 and CD4 staining (Fig 3, *A*). A distinct population of GZMB$^+$EOMES$^+$CD4 T cells was discerned within GC- and T-cell zones. Quantitative analysis using the QuPath software (Fig E2, *B* and *C*) revealed an expansion of EOMES$^+$GZMB$^+$CD4 T cells in both zones including GCs of CVIDc lymph nodes compared with non-CVID tonsils (Fig 3, *B*). There was no significant difference in the frequency of EOMES$^+$GZMB$^+$CD4 T cells between the CTLA-4–deficient patient and genetically undefined patients with CVIDc. Cytotoxic CD4$^+$ T cells were absent from the single CVIDio lymph node sample. In summary, increased amounts of cytotoxic CD4$^+$ T cells are located within GCs of CVIDc lymph nodes.

Only few of the cytotoxic T_{FH}-like CD4 T cells circulate in peripheral blood from patients with CVIDc

Because diagnostic access to SLOs from humans is limited, we set out to search for corresponding cytotoxic CD4 T-cell populations in peripheral blood reflecting the altered lymph node homeostasis in affected patients.

The same 44-marker CyTOF panel used in the analysis of the secondary lymphoid tissues was performed on peripheral blood cells from a cohort of overlapping patients with CVIDc and healthy donors (see Table E3). Dimensionality reduction and clustering by FlowSOM of all samples identified 31 unique clusters of CD4 T cells and revealed only partial overlap between peripheral blood and tissue-derived clusters (Fig 4, *A*; see also Fig E3, *A* and *B*, in this article's Online Repository at www.jacionline.org). Five cytotoxic clusters were identified in this analysis (Fig 4, *A* and *B*). Cluster 7 was exclusively present in blood and slightly increased in abundance between patients and controls (Fig 4, *B*). Because its phenotype differed strongly in regard to the expression of GC markers from the identified cytotoxic T-cell clusters in SLOs (Fig 4, *D*), we did not further investigate it. In contrast, cytotoxic clusters 27 and 29 were mainly found in secondary lymphoid tissues and nearly absent in peripheral blood of controls, with a significant expansion in patients with CVIDc when compared with controls (Fig 4, *B*). Cluster 27 resembles the cluster 2 previously identified in Fig 2 in regard to the expression of GC markers and the cytotoxic molecules reflecting also the reduced GZMA and GZMB expression when compared with the control group. Interestingly, cluster 29 behaves similarly, yet expresses sign of strong activation (Ki67 and HLA-DR), but unlike the clusters in the SLO, it is CD45RA-positive (Fig 4, *C* and *D*) and we suggest assigning this cluster to cytotoxic CD4 T_{EMRA} cells as previously described,[37] but the distinct phenotype does not allow to relate it with the expanded T_{HF} cluster in the lymph nodes of patients with CVIDc without further single-cell RNA-based termination of its trajectory.

Thus, the analysis of peripheral blood detected an expansion of cytotoxic CD4 T cells that are not related to the population identified in the SLO of the same patients. Cells that cluster with the cytotoxic cluster of the lymph node represent only a very small proportion of the circulating CD4 T cells.

DISCUSSION

The disturbed CD4 T-cell landscape in blood of patients with CVIDc frequently includes an expansion of circulating T_{FH}-like cells[18,38,39] and a shift from T_H2 toward T_H1 cells.[12,40] Circulating T_{FH}-like cells in CVIDc express more frequently exhaustion-associated markers such as TIGIT, TOX (thymocyte

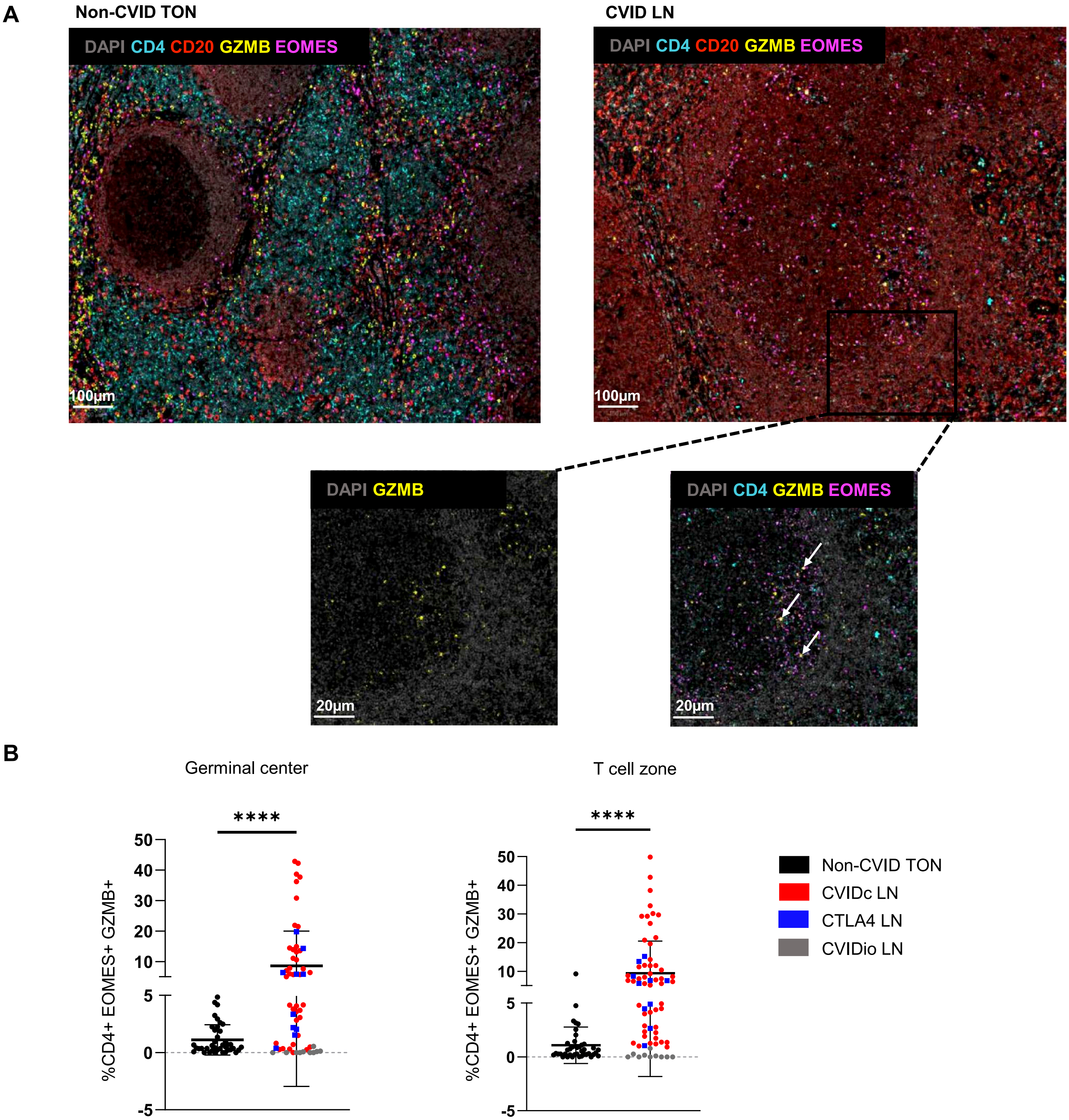

FIG 3. Increased infiltration of cytotoxic CD4$^+$EOMES$^+$GZMB$^+$ T cells in GCs of patients with CVIDc. **A,** Representative images of immunofluorescence (IF) staining for CD4 (*cyan*), CD20 (*red*), GZMB (*yellow*), EOMES (*magenta*), and DAPI (*gray*) in non-CVID tonsils (*left*) and CVIDc lymph nodes (*right*). *Arrowheads* indicate infiltrating CD4$^+$EOMES$^+$GZMB$^+$ T cells in the GC of a CVIDc lymph node. **B,** Percentage of CD4$^+$EOMES$^+$GZMB$^+$ T cells in GC and T-cell zones within non-CVID tonsils (n = 4) and CVID lymph nodes (n = 6). Each data point corresponds to 1 region of interest (GC or T-cell zone). Per tissue sample, 10 GCs and 10 T-cell zones were analyzed. The data points representing the CTLA-4–insufficient patient with CVIDc are highlighted in *blue*. The data points of the only patient with CVIDio are displayed in *gray*, but these were not considered in the statistical comparison of CVIDc vs non-CVID tissues. *DAPI*, 4′,6-Diamidino-2-phenylindol. For all plots, *P* values shown within each comparison were determined by the Mann-Whitney *U* test. **P* < .05; ***P* < .01; ****P* < .001; *****P* < .0001.

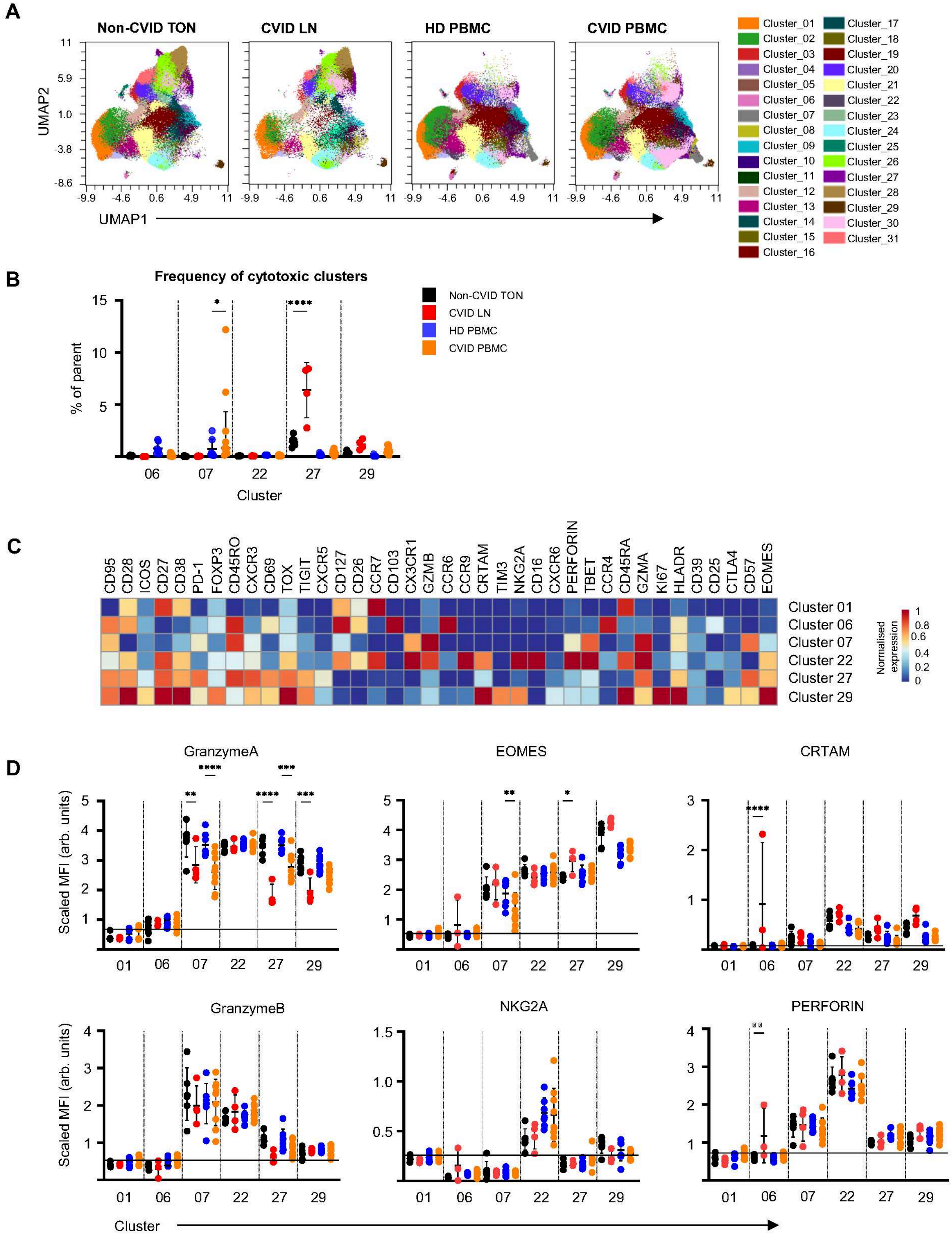

FIG 4. Low abundance of cytotoxic CD4 T_{FH}-like clusters in peripheral blood. **A,** UMAP projection of unsupervised CyTOF analysis of $CD4^+$ T cells from non-CVID tonsils (n = 5), CVIDc lymph nodes (n = 4), HD peripheral blood (n = 7), and CVIDc peripheral blood (n = 9). Clusters of similar cells were identified using FlowSOM. **B,** Abundance of cytotoxic clusters of interest in $CD4^+$ T cells (clusters 6, 7, 22, 27, and 29) in non-CVID tonsils (*black*), CVIDc lymph nodes (*red*), HD peripheral blood (*blue*), and CVID peripheral blood samples (*orange*). **C,** Heatmap of scaled expression values of markers analyzed with mass cytometry in cytotoxic clusters of interest (clusters 6, 7, 22, 27, and 29) compared with naive cells (cluster 1). **D,** Expression of cytotoxic markers GZMA, EOMES, CRTAM, GZMB, NKG2A, and perforin in naive cells (cluster 1) and clusters of interest (clusters 6, 7, 22, 27, and 29). MFI axis values are scaled by arcsinh, measured in arbitrary units. *HD,* Healthy donor; *MFI,* mean fluorescence intensitiy; *UMAP,* Uniform Manifold Approximation and Projection. For all plots, *P* values shown within each comparison were determined by the Mann-Whitney *U* test. $*P < .05$; $**P < .01$.

selection–associated HMG-box protein), PD-1, and CTLA-4, yet retain the capacity to produce IFN-γ and proliferate.[17,41] These changes in peripheral blood of patients with CVIDc most likely originate from alterations in secondary and possibly tertiary lymphoid tissues. Indeed, within ill-defined GCs of CVIDc-derived lymph nodes, a similar shift toward $T_{FH}1$ cells takes place,[12] but additional information on disturbances in T_{FH}-cell activation, differentiation, and fate is lacking from secondary lymphoid tissues of patients with CVIDc.

In this study, we used bulk RNA sequencing of sorted T_{FH} cells from lymph nodes of patients with CVIDc and tonsils of non-CVID immunocompetent controls to explore additional modifications contributing to the observed immunodeficiency and immune dysregulation. The transcriptome revealed not only elevated *TBX21*, *IFNG*, *CXCL10*, *GBP5*, and *ISG15*, reflecting the reported T_{FH1} expansion, but also for the first time an increased cytotoxic signature characterized by the increased expression of *CRTAM*, *GZMA*, *GZMK*, *PRF1*, *SLAMF7*, *NKG7*, *LYST*, and associated transcription factors *EOMES*, *ZEB2*, and *RUNX3* in CVIDc lymph nodes.[27-36] Therefore, we hypothesized that the increased cytotoxic signature derives from a specific T_{FH} subpopulation during the observed type 1 polarization in patients with CVIDc[12] because this has been reported previously during viral infections such as cytomegalovirus, EBV, HIV,[42-47] autoimmune disorders,[48-51] and malignant diseases[52-56] (for a review, see the study by Preglej and Ellmeier[57]). Despite some heterogeneity of the markers between different cytotoxic CD4 T cells, no profile currently indicates alternative function or the different clinical entities driving their expansion, which seems to reflect a shared potential CD4 T-cell differentiation pathway in a certain chronic cytokine environment.[57]

In the attempt to identify the source of this signature, CyTOF analysis of these CD4 T cells revealed distinct cytotoxic populations in secondary lymphoid tissues, confirming a heterogeneity of cytotoxic CD4 T cells.[57] Two clusters were enriched in CVIDc lymph nodes and 1 carried a CXCR5$^+$ICOS$^+$PD-1^{++} T_{FH} phenotype. This cluster was characterized by a CRTAM expression critical for the CTL differentiation of CD4 T cells and high expression of the transcription factors EOMES and T-bet together driving the expression of effector molecules such as perforin and granzymes, rendering them bona fide cytotoxic CD4 T_{FH} cells.[57,58] Interestingly, cluster 2 characterized by higher expression of EOMES, CRTAM, and GC-associated markers expresses increased activation markers (HLA-DR and slightly elevated Ki67) including elevated levels of FoxP3 and CD25 as has been previously described in a subtype of CD4 CTLs capable of killing various autologous cells.[59-61] This cluster also resembles the previously reported phenotypes (TIGIT, TOX, and PD-1) of circulating T_{FH} cells.[17,41]

Given the slightly lower expression of CXCR5 and PD-1 when compared with other T_{FH} cells from SLO, we wanted to ascertain that these cells locate into GCs. Multiplex immunofluorescence staining visualized an increase in EOMES$^+$GZMB$^+$ CD4 T cells not only in the T-cell zone but also in most GCs of the investigated CVIDc lymph nodes. Thus, on the basis of their location, this population most likely corresponds to cluster 2 of our CyTOF analysis in secondary lymphoid tissues.

Different signals have been implied in the expansion of cytotoxic CD4 T cells, including 4-1BB, IL-12 or type I and II interferon and IL-2, and Ox40[45,62,63] inducing T-bet, EOMES, and Blimp-1 expression in these cells. Although the presence of strong type II interferon signals in CVID lymph nodes is well established,[64] the presence of altered IL-2, 4-1BB, and OX40 signals still has to be shown. Persistent IL-12 stimulation of T_{FH} cells drives Zeb2$^+$ cytotoxic CD4 T cells in a *Salmonella enterica* model.[65] Interestingly, this was seen in the context of granuloma formation for the control of phagosomal pathogens,[65] possibly connecting the expansion of cytotoxic CD4 T cells with the frequent granulomatous lymphadenitis in patients with CVIDc.

In regard to function, cytotoxic CD4 T cells are reported to be multifunctional, including the production of different cytokines.[46] Their cytotoxic capacity was demonstrated in patients with HIV[66,67] and in patients with solid cancers and lymphoma.[68-70] Others found evidence for cytotoxic activity in blood-derived but little in tonsil-derived T_{FH} cells and yet speculated that these cells may contribute to the antibody deficiency and immune dysregulation in CTLA-4 haploinsufficiency.[71] Our preliminary *ex vivo* investigations of CVIDc lymph node–derived cytotoxic CD4 cells suggest that the reduced intracellular content of cytotoxic molecules and therefore potentially reduced cytotoxic activity *in vitro* might be due to preceding active release of these molecules by degranulation *in vivo* as indicated by elevated surface expression of CD107a. This would be an alternative explanation for the observed reduction in cytotoxic molecules in tissue-derived cytotoxic CD4 T cells than chronic exhaustion, which would not be associated with elevated transcript levels for these molecules or surface expression of CD107a.[72] Elevated expression of CD107a as a marker for the fusion of lytic granules with the plasma membrane in cytotoxic CD4 T cells has also been described in the context of viral, autoimmune, and malignant disease.[57] Therefore, the cytotoxic CD4 T cells we identified in CVIDc lymph nodes are not only highly activated but also appear to actively release cytotoxic granules. This interpretation would explain the discrepancy between elevated RNA message and reduced protein content of these molecules. Such a cytotoxic activity might interfere with the efficient production of long-term memory B cells in GCs as speculated during severe acute respiratory syndrome coronavirus 2 infection, wherein the authors suggested that circulating cytotoxic CD4 T_{FH} cells might be involved in the observed loss of GC in lymph nodes and a subsequently impaired humoral immunity.[73] The B-cell–promoting function of Zeb2$^+$ age-associated CD4 T cells as identified in systemic lupus erythematosus does not seem to apply for CVID-derived secondary lymphoid tissues.[29] Further investigation is required to determine whether in CVIDc an infection-driven expansion of cytotoxic CD4 T cells as observed in severe acute respiratory syndrome coronavirus 2 infection contributes to a secondary failure of the GC reaction because CD4 T_{FH} CTLs might kill B cells, activated MHC II–positive T cells, dendritic cells, and macrophages.[60,74,75]

In the investigated patients there was no malignancy detected. Therefore, it is tempting to speculate that recurrent T-cell stimulation in the context of chronic, replicating (viral) infections[28] is a conceivable cause for the expansion of these cells in patients with CVIDc. Autoimmunity and chronic inflammation represent an obvious alternative trigger especially in genetically defined CVID-like disorders such as CTLA-4 haploinsufficiency, but might also be a consequence of the expansion of the cytotoxic subsets in patients with CVIDc because it has been assumed for coronavirus disease 2019–associated lung disease.[76]

Although this study had the unique opportunity to investigate human secondary lymphoid tissues of patients with CVIDc and revealed another facet of the immune dysregulation in these patients, there are clear limitations. We could examine only a small group of patients, restricted to patients with CVIDc with lymphadenopathy, necessitating the removal of a lymph node for the exclusion of lymphoma. Although it is intriguing to observe a similar expansion of the cytotoxic T_{FH} cells in the single patient with NFKB1 haploinsufficiency and the one with CTLA-4 insufficiency because it suggests that both monogenetic CVID-like disorders might share this common pathway of pathogenesis, additional samples are required to confirm this hypothesis. This finding would support the idea that primary causes of a disturbed GC function may still use common effector mechanisms driving the observed pathology that could be targeted. The restricted access to this material and the very low number of circulating cytotoxic T_{FH} cells hinder also the performance of substantial functional studies to demonstrate the hypothesized role of these cells in the observed GC failure in patients with CVID. Unfortunately, our own attempts to demonstrate that CD4 CTLs of patients with CVIDc can kill autologous GC B cells *in vitro* and the investigation of elevated unstimulated expression of CD107a were hampered by the limited residual cell material. Future studies need to address this and the heterogeneity of this population with additional functional assays and more granular transcriptomic technologies, such as single-cell RNA sequencing and cell trajectory analysis. These studies will also need to address the additional factors in patients with CVIDc leading to the combination of hypogammaglobulinemia and immune dysregulation, which is not seen to the same extent in systemic lupus erythematosus or certain chronic viral infections in which a similar expansion has been observed.

We describe for the first time that the type 1 polarization of the GC landscape in lymph nodes of patients with CVIDc is associated with an expansion of cytotoxic CD4 T_{FH}-cell populations. This includes a strongly activated population that resembles cytotoxic CD4 T-cell populations observed in viral infection, autoimmunity, and malignancy.[57] The role of these potentially multifunctional cytotoxic CD4 T cells within the complex dysregulation of the immune system of CVIDc deserves more attention because it might highlight aspects of a shared pathogenesis of the altered GC function and it will educate us about the risk and benefit of targeted therapies and use of checkpoint inhibitors in patients with CVIDc.

DISCLOSURE STATEMENT

This study was supported by the German Federal Ministry of Education and Research (BMBF; 01EO1303). K.W. received funding by the BMBF Netzwerke Seltener Erkrankungen (GAIN 01GM2206A) and the Deutsche Forschungsgemeinschaft (DFG) SFB1160 IMPATH (project A04). This study was also supported by the DFG, Germany, SFB1160 IMPATH (project ID 256073931) and the German Mass Cytometry Alliance (project ID 518316185) and Heisenberg grant (project ID 520992132) to B.B. A.E.S was supported by the MOTI-VATE program of the Medical Faculty, University of Freiburg. T.B. was supported by an Excellence Fellowship from the Else Kröner-Fresenius-Foundation. B.K. received funding by the DFG (project ID 545533246). The study received funding from the EU-H2020-MSCA-COFUND EURIdoc programme (no. 101034170 to K.W.) and the support by the Open Access Publication Fund of the University of Freiburg. It also received funding from the DFG within the CRC1160 (project ID 256073931-Z02 to M.B.), CRC/TRR167 (project ID 259373024-Z01 to M.B.), CRC1453 (project ID 431984000-S1 to M.B.), and CRC1479 (project ID 441891347-S1 to M.B.) and funding from the BMBF within the Medical Informatics Funding Scheme, MIRACUM–FKZ 01ZZ1801B and PM4Onco–FKZ 01ZZ2322A (to M.B.) and EkoEstMed–FKZ 01ZZ2015 (to G.A.). A.K. was supported by a grant from the Czech Health Research Council and Ministry of Health, Czech Republic (grant no. AZV NU23-05-00097). C.S. received funding from the DFG (DFG SFB IMPATH–INST39/987-3, Z01, and SCHE2092/5-1).

Disclosure of potential conflict of interest: The authors declare that they have no relevant conflicts of interest.

We thank Ed Pearce for mentoring David Friedmann and the discussion of the study. Some samples for this project were obtained from the Center for Chronic Immunodeficiency Biobank, which is a partner biobank/hub of the University Medical Center Freiburg and Medical Faculty "Center for Biobanking—FREEZE." We thank the physicians, study nurses, and patients of the Center for Chronic Immunodeficiency and the Department of Rheumatology and Clinical Immunology of the University Medical Center Freiburg for patient care and support. We acknowledge the Lighthouse Core Facility unit for their excellent assistance with cell sorting and flow cytometry and Patricia Otto-Mora and Jürgen Beck for operating the CyTOF and data acquisition. Some figures were created with BioRender.com.

Key message

- **T_{FH} cells in CVIDc lymph nodes comprise an expansion of a cytotoxic CRTAM$^+$T-bet$^+$EOMES$^+$GZMA$^+$ Perforin$^+$CD4 T-cell cluster, which is only poorly reflected in peripheral blood.**

REFERENCES

1. Seidel MG, Kindle G, Gathmann B, Quinti I, Buckland M, van Montfrans J, et al. The European Society for Immunodeficiencies (ESID) Registry working definitions for the clinical diagnosis of inborn errors of immunity. J Allergy Clin Immunol Pract 2019;7:1763-70.
2. Bonilla FA, Barlan I, Chapel H, Costa-Carvalho BT, Cunningham-Rundles C, de la Morena MT, et al. International Consensus Document (ICON): common variable immunodeficiency disorders. J Allergy Clin Immunol Pract 2016;4:38-59.
3. Tuijnenburg P, Lango Allen H, Burns SO, Greene D, Jansen MH, Staples E, et al. Loss-of-function nuclear factor kappaB subunit 1 (NFKB1) variants are the most common monogenic cause of common variable immunodeficiency in Europeans. J Allergy Clin Immunol 2018;142:1285-96.
4. Aggarwal V, Banday AZ, Jindal AK, Das J, Rawat A. Recent advances in elucidating the genetics of common variable immunodeficiency. Genes Dis 2020;7:26-37.
5. Chapel H, Lucas M, Patel S, Lee M, Cunningham-Rundles C, Resnick E, et al. Confirmation and improvement of criteria for clinical phenotyping in common variable immunodeficiency disorders in replicate cohorts. J Allergy Clin Immunol 2012;130:1197-8.e9.
6. Chapel H, Lucas M, Lee M, Bjorkander J, Webster D, Grimbacher B, et al. Common variable immunodeficiency disorders: division into distinct clinical phenotypes. Blood 2008;112:277-86.
7. Resnick ES, Cunningham-Rundles C. The many faces of the clinical picture of common variable immune deficiency. Curr Opin Allergy Clin Immunol 2012;12:595-601.
8. Rider NL, Kutac C, Hajjar J, Scalchunes C, Seeborg FO, Boyle M, et al. Health-related quality of life in adult patients with common variable immunodeficiency disorders and impact of treatment. J Clin Immunol 2017;37:461-75.
9. Bayrhuber M, Tinsel I, Goldacker S, Kindle G, Warnatz K, Farin E, et al. Perceived health of patients with common variable immunodeficiency—a cluster analysis. Clin Exp Immunol 2019;196:76-85.
10. Wehr C, Kivioja T, Schmitt C, Ferry B, Witte T, Eren E, et al. The EUROclass trial: defining subgroups in common variable immunodeficiency. Blood 2008;111:77-85.

11. Unger S, Seidl M, Schmitt-Graeff A, Bohm J, Schrenk K, Wehr C, et al. Ill-defined germinal centers and severely reduced plasma cells are histological hallmarks of lymphadenopathy in patients with common variable immunodeficiency. J Clin Immunol 2014;34:615-26.
12. Unger S, Seidl M, van Schouwenburg P, Rakhmanov M, Bulashevska A, Frede N, et al. The T(H)1 phenotype of follicular helper T cells indicates an IFN-gamma-associated immune dysregulation in patients with CD21low common variable immunodeficiency. J Allergy Clin Immunol 2018;141:730-40.
13. Klocperk A, Unger S, Friedmann D, Seidl M, Zoldan K, Pfeiffer J, et al. Exhausted phenotype of follicular CD8 T cells in CVID. J Allergy Clin Immunol 2020;146:912-5.e13.
14. Klocperk A, Friedmann D, Schlaak AE, Unger S, Parackova Z, Goldacker S, et al. Distinct CD8 T cell populations with differential exhaustion profiles associate with secondary complications in common variable immunodeficiency. J Clin Immunol 2022;42:1254-69.
15. Giovannetti A, Pierdominici M, Mazzetta F, Marziali M, Renzi C, Mileo AM, et al. Unravelling the complexity of T cell abnormalities in common variable immunodeficiency. J Immunol 2007;178:3932-43.
16. Guazzi V, Aiuti F, Mezzaroma I, Mazzetta F, Andolfi G, Mortellaro A, et al. Assessment of thymic output in common variable immunodeficiency patients by evaluation of T cell receptor excision circles. Clin Exp Immunol 2002;129:346-53.
17. Berbers RM, van der Wal MM, van Montfrans JM, Ellerbroek PM, Dalm V, van Hagen PM, et al. Chronically activated T-cells retain their inflammatory properties in common variable immunodeficiency. J Clin Immunol 2021;41:1621-32.
18. Romberg N, Le Coz C, Glauzy S, Schickel JN, Trofa M, Nolan BE, et al. Patients with common variable immunodeficiency with autoimmune cytopenias exhibit hyperplastic yet inefficient germinal center responses. J Allergy Clin Immunol 2019;143:258-65.
19. Bolger AM, Lohse M, Usadel B. Trimmomatic: a flexible trimmer for Illumina sequence data. Bioinformatics 2014;30:2114-20.
20. Dobin A, Davis CA, Schlesinger F, Drenkow J, Zaleski C, Jha S, et al. STAR: ultrafast universal RNA-seq aligner. Bioinformatics 2013;29:15-21.
21. Ritchie ME, Phipson B, Wu D, Hu Y, Law CW, Shi W, et al. limma powers differential expression analyses for RNA-sequencing and microarray studies. Nucleic Acids Res 2015;43:e47.
22. Wu T, Hu E, Xu S, Chen M, Guo P, Dai Z, et al. clusterProfiler 4.0: a universal enrichment tool for interpreting omics data. Innovation (Camb) 2021;2:100141.
23. Subramanian A, Tamayo P, Mootha VK, Mukherjee S, Ebert BL, Gillette MA, et al. Gene set enrichment analysis: a knowledge-based approach for interpreting genome-wide expression profiles. Proc Natl Acad Sci U S A 2005;102:15545-50.
24. Schulz AR, Mei HE. Surface barcoding of live PBMC for multiplexed mass cytometry. Methods Mol Biol 2019;1989:93-108.
25. Van Gassen S, Callebaut B, Van Helden MJ, Lambrecht BN, Demeester P, Dhaene T, et al. FlowSOM: using self-organizing maps for visualization and interpretation of cytometry data. Cytometry A 2015;87:636-45.
26. Becht E, McInnes L, Healy J, Dutertre CA, Kwok IWH, Ng LG, et al. Dimensionality reduction for visualizing single-cell data using UMAP [published online ahead of print December 3, 2018]. Nat Biotechnol. https://doi.org/10.1038/nbt.4314.
27. Serroukh Y, Gu-Trantien C, Hooshiar Kashani B, Defrance M, Vu Manh TP, Azouz A, et al. The transcription factors Runx3 and ThPOK cross-regulate acquisition of cytotoxic function by human Th1 lymphocytes. eLife 2018;7:e30496.
28. Knudson CJ, Férez M, Alves-Peixoto P, Erkes DA, Melo-Silva CR, Tang L, et al. Mechanisms of antiviral cytotoxic CD4 T cell differentiation. J Virol 2021;95:e0056621.
29. Goto M, Takahashi H, Yoshida R, Itamiya T, Nakano M, Nagafuchi Y, et al. Age-associated CD4(+) T cells with B cell-promoting functions are regulated by ZEB2 in autoimmunity. Sci Immunol 2024;9:eadk1643.
30. Takeuchi A, Badr Mel S, Miyauchi K, Ishihara C, Onishi R, Guo Z, et al. CRTAM determines the CD4+ cytotoxic T lymphocyte lineage. J Exp Med 2016;213:123-38.
31. Wang X, Xiong H, Ning Z. Implications of NKG2A in immunity and immune-mediated diseases. Front Immunol 2022;13:960852.
32. Lei Y, Takahama Y. XCL1 and XCR1 in the immune system. Microbes Infect 2012;14:262-7.
33. Gutierrez-Guerrero A, Mancilla-Herrera I, Maravillas-Montero JL, Martinez-Duncker I, Veillette A, Cruz-Munoz ME. SLAMF7 selectively favors degranulation to promote cytotoxicity in human NK cells. Eur J Immunol 2022;52:62-74.
34. Della-Torre E, Bozzalla-Cassione E, Sciorati C, Ruggiero E, Lanzillotta M, Bonfiglio S, et al. A CD8alpha- subset of CD4+SLAMF7+ cytotoxic T cells is expanded in patients with IgG4-related disease and decreases following glucocorticoid treatment. Arthritis Rheumatol 2018;70:1133-43.
35. Ng SS, De Labastida Rivera F, Yan J, Corvino D, Das I, Zhang P, et al. The NK cell granule protein NKG7 regulates cytotoxic granule exocytosis and inflammation. Nat Immunol 2020;21:1205-18.
36. Gil-Krzewska A, Wood SM, Murakami Y, Nguyen V, Chiang SCC, Cullinane AR, et al. Chediak-Higashi syndrome: lysosomal trafficking regulator domains regulate exocytosis of lytic granules but not cytokine secretion by natural killer cells. J Allergy Clin Immunol 2016;137:1165-77.
37. Patil VS, Madrigal A, Schmiedel BJ, Clarke J, O'Rourke P, de Silva AD, et al. Precursors of human CD4(+) cytotoxic T lymphocytes identified by single-cell transcriptome analysis. Sci Immunol 2018;3:eaan8664.
38. Coraglia A, Galassi N, Fernández Romero DS, Juri MC, Felippo M, Malbrán A, et al. Common variable immunodeficiency and circulating TFH. J Immunol Res 2016;2016:4951587.
39. Edwards ESJ, Bosco JJ, Aui PM, Stirling RG, Cameron PU, Chatelier J, et al. Predominantly antibody-deficient patients with non-infectious complications have reduced naive B, Treg, Th17, and Tfh17 cells. Front Immunol 2019;10:2593.
40. Turpin D, Furudoi A, Parrens M, Blanco P, Viallard JF, Duluc D. Increase of follicular helper T cells skewed toward a Th1 profile in CVID patients with non-infectious clinical complications. Clin Immunol 2018;197:130-8.
41. Milardi G, Di Lorenzo B, Gerosa J, Barzaghi F, Di Matteo G, Omrani M, et al. Follicular helper T cell signature of replicative exhaustion, apoptosis, and senescence in common variable immunodeficiency. Eur J Immunol 2022;52:1171-89.
42. Zaunders JJ, Dyer WB, Wang B, Munier ML, Miranda-Saksena M, Newton R, et al. Identification of circulating antigen-specific CD4+ T lymphocytes with a CCR5+, cytotoxic phenotype in an HIV-1 long-term nonprogressor and in CMV infection. Blood 2004;103:2238-47.
43. van Leeuwen EM, Remmerswaal EB, Vossen MT, Rowshani AT, Wertheim-van Dillen PM, van Lier RA, et al. Emergence of a CD4+CD28− granzyme B+, cytomegalovirus-specific T cell subset after recovery of primary cytomegalovirus infection. J Immunol 2004;173:1834-41.
44. Wilkinson TM, Li CK, Chui CS, Huang AK, Perkins M, Liebner JC, et al. Preexisting influenza-specific CD4+ T cells correlate with disease protection against influenza challenge in humans. Nat Med 2012;18:274-80.
45. Hua L, Yao S, Pham D, Jiang L, Wright J, Sawant D, et al. Cytokine-dependent induction of CD4+ T cells with cytotoxic potential during influenza virus infection. J Virol 2013;87:11884-93.
46. Brown DM, Lee S, Garcia-Hernandez Mde L, Swain SL. Multifunctional CD4 cells expressing gamma interferon and perforin mediate protection against lethal influenza virus infection. J Virol 2012;86:6792-803.
47. Haigh TA, Lin X, Jia H, Hui EP, Chan AT, Rickinson AB, et al. EBV latent membrane proteins (LMPs) 1 and 2 as immunotherapeutic targets: LMP-specific CD4+ cytotoxic T cell recognition of EBV-transformed B cell lines. J Immunol 2008;180:1643-54.
48. Namekawa T, Wagner UG, Goronzy JJ, Weyand CM. Functional subsets of CD4 T cells in rheumatoid synovitis. Arthritis Rheum 1998;41:2108-16.
49. Thewissen M, Somers V, Hellings N, Fraussen J, Damoiseaux J, Stinissen P. CD4+CD28null T cells in autoimmune disease: pathogenic features and decreased susceptibility to immunoregulation. J Immunol 2007;179:6514-23.
50. Hong X, Meng S, Tang D, Wang T, Ding L, Yu H, et al. Single-cell RNA sequencing reveals the expansion of cytotoxic CD4(+) T lymphocytes and a landscape of immune cells in primary Sjogren's syndrome. Front Immunol 2020;11:594658.
51. Yang D, Tian Z, Zhang M, Yang W, Tang J, Wu Y, et al. NKG2D(+)CD4(+) T cells kill regulatory T cells in a NKG2D-NKG2D ligand-dependent manner in systemic lupus erythematosus. Sci Rep 2017;7:1288.
52. Cachot A, Bilous M, Liu YC, Li X, Saillard M, Cenerenti M, et al. Tumor-specific cytolytic CD4 T cells mediate immunity against human cancer. Sci Adv 2021;7:eabe3348.
53. Guo X, Zhang Y, Zheng L, Zheng C, Song J, Zhang Q, et al. Global characterization of T cells in non-small-cell lung cancer by single-cell sequencing. Nat Med 2018;24:978-85.
54. Zhang Q, He Y, Luo N, Patel SJ, Han Y, Gao R, et al. Landscape and dynamics of single immune cells in hepatocellular carcinoma. Cell 2019;179:829-45.e20.
55. Zheng C, Zheng L, Yoo JK, Guo H, Zhang Y, Guo X, et al. Landscape of infiltrating T cells in liver cancer revealed by single-cell sequencing. Cell 2017;169:1342-56.e16.
56. Zhou Y, Yang D, Yang Q, Lv X, Huang W, Zhou Z, et al. Single-cell RNA landscape of intratumoral heterogeneity and immunosuppressive microenvironment in advanced osteosarcoma. Nat Commun 2020;11:6322.
57. Preglej T, Ellmeier W. CD4(+) cytotoxic T cells—phenotype, function and transcriptional networks controlling their differentiation pathways. Immunol Lett 2022;247:27-42.
58. Eshima K, Misawa K, Ohashi C, Iwabuchi K. Role of T-bet, the master regulator of Th1 cells, in the cytotoxicity of murine CD4(+) T cells. Microbiol Immunol 2018;62:348-56.

59. Cao X, Cai SF, Fehniger TA, Song J, Collins LI, Piwnica-Worms DR, et al. Granzyme B and perforin are important for regulatory T cell-mediated suppression of tumor clearance. Immunity 2007;27:635-46.
60. Grossman WJ, Verbsky JW, Barchet W, Colonna M, Atkinson JP, Ley TJ. Human T regulatory cells can use the perforin pathway to cause autologous target cell death. Immunity 2004;21:589-601.
61. Zhao DM, Thornton AM, DiPaolo RJ, Shevach EM. Activated CD4+CD25+ T cells selectively kill B lymphocytes. Blood 2006;107:3925-32.
62. Akhmetzyanova I, Zelinskyy G, Littwitz-Salomon E, Malyshkina A, Dietze KK, Streeck H, et al. CD137 agonist therapy can reprogram regulatory T cells into cytotoxic CD4+ T cells with antitumor activity. J Immunol 2016;196:484-92.
63. Hirschhorn-Cymerman D, Budhu S, Kitano S, Liu C, Zhao F, Zhong H, et al. Induction of tumoricidal function in CD4+ T cells is associated with concomitant memory and terminally differentiated phenotype. J Exp Med 2012;209:2113-26.
64. Unger S, Seidl M, van Schouwenburg P, Rakhmanov M, Bulashevska A, Frede N, et al. The T(H)1 phenotype of follicular helper T cells indicates an IFN-γ-associated immune dysregulation in patients with CD21low common variable immunodeficiency. J Allergy Clin Immunol 2018;141:730-40.
65. Krueger PD, Goldberg MF, Hong SW, Osum KC, Langlois RA, Kotov DI, et al. Two sequential activation modules control the differentiation of protective T helper-1 (Th1) cells. Immunity 2021;54:687-701.e4.
66. Appay V, Zaunders JJ, Papagno L, Sutton J, Jaramillo A, Waters A, et al. Characterization of CD4(+) CTLs ex vivo. J Immunol 2002;168:5954-8.
67. Soghoian DZ, Jessen H, Flanders M, Sierra-Davidson K, Cutler S, Pertel T, et al. HIV-specific cytolytic CD4 T cell responses during acute HIV infection predict disease outcome. Sci Transl Med 2012;4:123ra25.
68. Quezada SA, Simpson TR, Peggs KS, Merghoub T, Vider J, Fan X, et al. Tumor-reactive CD4(+) T cells develop cytotoxic activity and eradicate large established melanoma after transfer into lymphopenic hosts. J Exp Med 2010;207:637-50.
69. Khanna R, Burrows SR, Thomson SA, Moss DJ, Cresswell P, Poulsen LM, et al. Class I processing-defective Burkitt's lymphoma cells are recognized efficiently by CD4+ EBV-specific CTLs. J Immunol 1997;158:3619-25.
70. Porakishvili N, Kardava L, Jewell AP, Yong K, Glennie MJ, Akbar A, et al. Cytotoxic CD4+ T cells in patients with B cell chronic lymphocytic leukemia kill via a perforin-mediated pathway. Haematologica 2004;89:435-43.
71. Hao Y, Miraghazadeh B, Chand R, Davies AR, Cardinez C, Kwong K, et al. CTLA4 protects against maladaptive cytotoxicity during the differentiation of effector and follicular CD4(+) T cells. Cell Mol Immunol 2023;20:777-93.
72. Alshekaili J, Chand R, Lee CE, Corley S, Kwong K, Papa I, et al. STAT3 regulates cytotoxicity of human CD57+ CD4+ T cells in blood and lymphoid follicles. Sci Rep 2018;8:3529.
73. Meckiff BJ, Ramirez-Suastegui C, Fajardo V, Chee SJ, Kusnadi A, Simon H, et al. Imbalance of regulatory and cytotoxic SARS-CoV-2-reactive CD4(+) T cells in COVID-19. Cell 2020;183:1340-53.e16.
74. Mauri D, Wyss-Coray T, Gallati H, Pichler WJ. Antigen-presenting T cells induce the development of cytotoxic CD4+ T cells. I. Involvement of the CD80-CD28 adhesion molecules. J Immunol 1995;155:118-27.
75. Adhikary D, Damaschke J, Mautner J, Behrends U. The Epstein-Barr virus major tegument protein BNRF1 is a common target of cytotoxic CD4(+) T cells. J Virol 2020;94:e00284-20.
76. Kaneko N, Boucau J, Kuo HH, Perugino C, Mahajan VS, Farmer JR, et al. Temporal changes in T cell subsets and expansion of cytotoxic CD4+ T cells in the lungs in severe COVID-19. Clin Immunol 2022;237:108991.